A fragment profiling approach to inhibitors of the orphan *M. tuberculosis* P450 CYP144A1

*Madeline E. Kavanagh,[a] Jude Chenge,[b†] Azedine Zoufir,[a] Kirsty J. McLean,[b] Anthony, G. Coyne,[a] Andreas Bender,[a] Andrew W. Munro[b] and Chris Abell[a]**

[a]Department of Chemistry, University of Cambridge, Lensfield Road, Cambridge CB2 1EW, United Kingdom; [b]Centre for Synthetic Biology of Fine and Specialty Chemicals (SYNBIOCHEM), Manchester Institute of Biotechnology, School of Chemistry, The University of Manchester, Manchester M1 7DN, United Kingdom.

*Corresponding author: Chris Abell, ca26@cam.ac.uk

Keywords: fragment screening, ligand profile, cytochrome P450 enzyme, *Mycobacterium tuberculosis*, CYP144A1

Supporting Information

Table S1. Fragment profile similarity of *Mtb* cytochrome P450 enzymes determined from screening an unbiased, rule-of-three compliant fragment library by ligand-observed NMR. Profiles calculated to be significantly similar have been shaded grey.

Enzyme 1	Enzyme 2	E-value	P-value
CYP121A1	CYP144A1	3.0E-07	3.0E-07
CYP125A1	CYP142A1	3.7E-06	3.7E-06
CYP124A1	CYP142A1	5.6E-06	5.6E-06
CYP124A1	CYP125A1	3.1E-05	3.1E-05
CYP121A1	CYP125A1	7.6E-05	7.6E-05
CYP121A1	CYP124A1	2.2E-04	2.2E-04
CYP142A1	CYP126A1	2.4E-04	2.4E-04
CYP124A1	CYP144A1	3.0E-04	3.0E-04
CYP121A1	CYP126A1	4.3E-04	4.3E-04
CYP124A1	CYP126A1	5.4E-04	5.4E-04
CYP121A1	CYP143A1	6.0E-04	6.0E-04
CYP125A1	CYP126A1	9.2E-04	9.2E-04
CYP125A1	CYP144A1	1.6E-03	1.6E-03
CYP121A1	CYP142A1	2.3E-03	2.2E-03
CYP142A1	CYP144A1	4.9E-03	4.9E-03
CYP144A1	CYP143A1	5.4E-03	5.3E-03
CYP144A1	CYP126A1	6.9E-03	6.9E-03
CYP125A1	CYP143A1	1.5E-02	1.5E-02
CYP126A1	CYP143A1	4.4E-02	4.3E-02
CYP142A1	CYP143A1	4.5E-02	4.4E-02
CYP124A1	CYP143A1	6.6E-02	6.4E-02

Table S2. Fragment profile similarity of *Mtb* cytochrome P450 enzymes determined from screening a focused library of heme-binding fragments by UV-vis spectroscopy. Profiles calculated to be significantly similar have been shaded grey.

Enzyme 1	Enzyme 2	E-value	P-value
CYP102A1 HD WT	CYP102A1 HD A82F	8.2E-07	8.2E-07
CYP142A1	CYP102A1 HD A82F	9.3E-06	9.3E-06
CYP124A1	CYP142A1	8.6E-05	8.6E-05
CYP142A1	CYP102A1 HD WT	1.6E-04	1.6E-04
CYP124A1	CYP105AS1	1.7E-04	1.7E-04
CYP152L1	CYP105AS1	7.5E-04	7.5E-04
CYP121A1	CYP126A1	1.5E-03	1.5E-03
CYP102A1 HD WT	CYP105AS1	1.8E-03	1.8E-03
CYP124A1	CYP102A1 HD A82F	1.8E-03	1.8E-03
CYP125A1	CYP144A1	2.5E-03	2.5E-03
CYP142A1	CYP152L1	2.9E-03	2.8E-03
CYP124A1	CYP152L1	3.0E-03	3.0E-03
CYP102A1 HD A82F	CYP105AS1	3.5E-03	3.5E-03

CYP121A1	CYP144A1	3.8E-03	3.7E-03
CYP124A1	CYP102A1 HD WT	3.8E-03	3.7E-03
CYP125A1	CYP126A1	5.3E-03	5.3E-03
CYP125A1	CYP143A1	5.3E-03	5.3E-03
CYP102A1 HD WT	CYP152L1	5.9E-03	5.9E-03
CYP126A1	CYP142A1	6.0E-03	5.9E-03
CYP142A1	CYP143A1	6.0E-03	5.9E-03
CYP142A1	CYP105AS1	6.5E-03	6.5E-03
CYP102A1 HD A82F	CYP152L1	9.9E-03	9.8E-03
CYP124A1	CYP143A1	1.2E-02	1.2E-02
CYP124A1	CYP125A1	1.2E-02	1.2E-02
CYP143A1	CYP105AS1	1.6E-02	1.6E-02
CYP143A1	CYP102A1 HD A82F	2.0E-02	2.0E-02
CYP126A1	CYP152L1	2.5E-02	2.5E-02
CYP143A1	CYP152L1	2.5E-02	2.5E-02
CYP125A1	CYP142A1	2.6E-02	2.6E-02
CYP125A1	CYP102A1 HD A82F	2.8E-02	2.8E-02
CYP126A1	CYP102A1 HD WT	3.0E-02	3.0E-02
CYP143A1	CYP102A1 HD WT	3.0E-02	3.0E-02
CYP126A1	CYP143A1	3.1E-02	3.0E-02
CYP121A1	CYP125A1	3.3E-02	3.2E-02
CYP121A1	CYP124A1	3.3E-02	3.2E-02
CYP125A1	CYP102A1 HD WT	3.7E-02	3.6E-02
CYP121A1	CYP152L1	5.4E-02	5.3E-02
CYP126A1	CYP102A1 HD A82F	5.8E-02	5.6E-02
CYP124A1	CYP126A1	5.9E-02	5.8E-02
CYP121A1	CYP102A1 HD WT	6.1E-02	6.0E-02
CYP121A1	CYP142A1	6.2E-02	6.0E-02
CYP125A1	CYP152L1	6.3E-02	6.1E-02
CYP126A1	CYP105AS1	6.9E-02	6.7E-02
CYP126A1	CYP144A1	8.1E-02	7.8E-02
CYP143A1	CYP144A1	8.1E-02	7.8E-02
CYP121A1	CYP102A1 HD A82F	8.6E-02	8.3E-02
CYP125A1	CYP105AS1	8.8E-02	8.4E-02
CYP121A1	CYP143A1	9.6E-02	9.2E-02
CYP124A1	CYP144A1	1.0E-01	9.7E-02
CYP144A1	CYP105AS1	1.1E-01	1.0E-01
CYP144A1	CYP152L1	1.2E-01	1.1E-01
CYP121A1	CYP105AS1	1.2E-01	1.2E-01
CYP142A1	CYP144A1	1.2E-01	1.2E-01
CYP144A1	CYP102A1 HD WT	1.4E-01	1.3E-01
CYP144A1	CYP102A1 HD A82F	1.5E-01	1.4E-01

Table S3. Potential substrates screened against *Mtb* CYP144A1 using UV-vis spectroscopy and in biochemical assays. The protocol for UV-vis screening is described in the main paper. Biochemical assays were performed according to the previously reported procedure, (Driscoll *et al., J. Biol. Chem.* **2010**, 285:38270–38282) using 1 mM compounds, 0.5 μM CYP144A1 in 50 mM KPi (pH 7.0), 10 μM spinach ferredoxin, 10 μM spinach ferredoxin reductase, 1 mM NADPH and an internal NADPH regenerating system of glucose-6-phosphate/glucose-6-phosphate dehydrogenase. Control assays omitting CYP144A1 were also run.

Indazole **1** was the only compound to produce type I perturbations in the optical spectrum of CYP144A1. No oxidation products were detected for any compounds in LCMS traces.

Compounds analyzed by UV-vis and in biochemical assays		
Indazole **1**		
Cholesterol	Myristic acid	D-sphigosine
Cholestenone	Pentadecanoic acid	D-glucose
Testosterone	Palmitoleic acid	**D**-mannose
Vitamin D	Arachidonic acid	**D**-fructose
Phytanic acid	Parinaric acid	Maltose
Biotin	Arachidic acid	Galactose
Vitamin K	Tridecanoic acid	starch

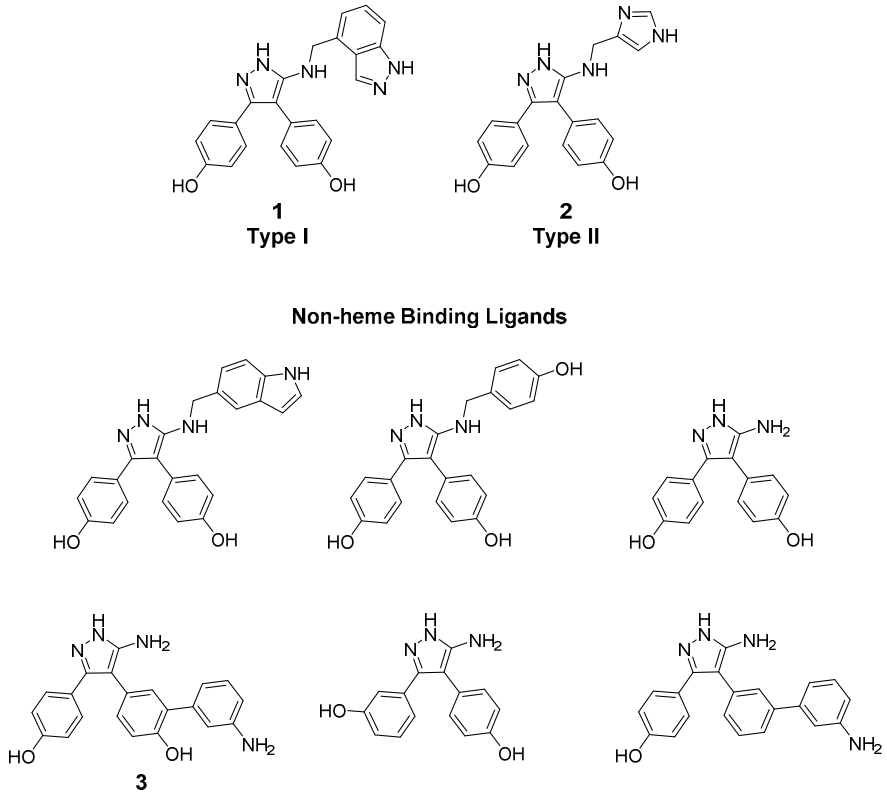

Figure S1. CYP144A1 ligands that were identified from a library of CYP121A1 inhibitors.

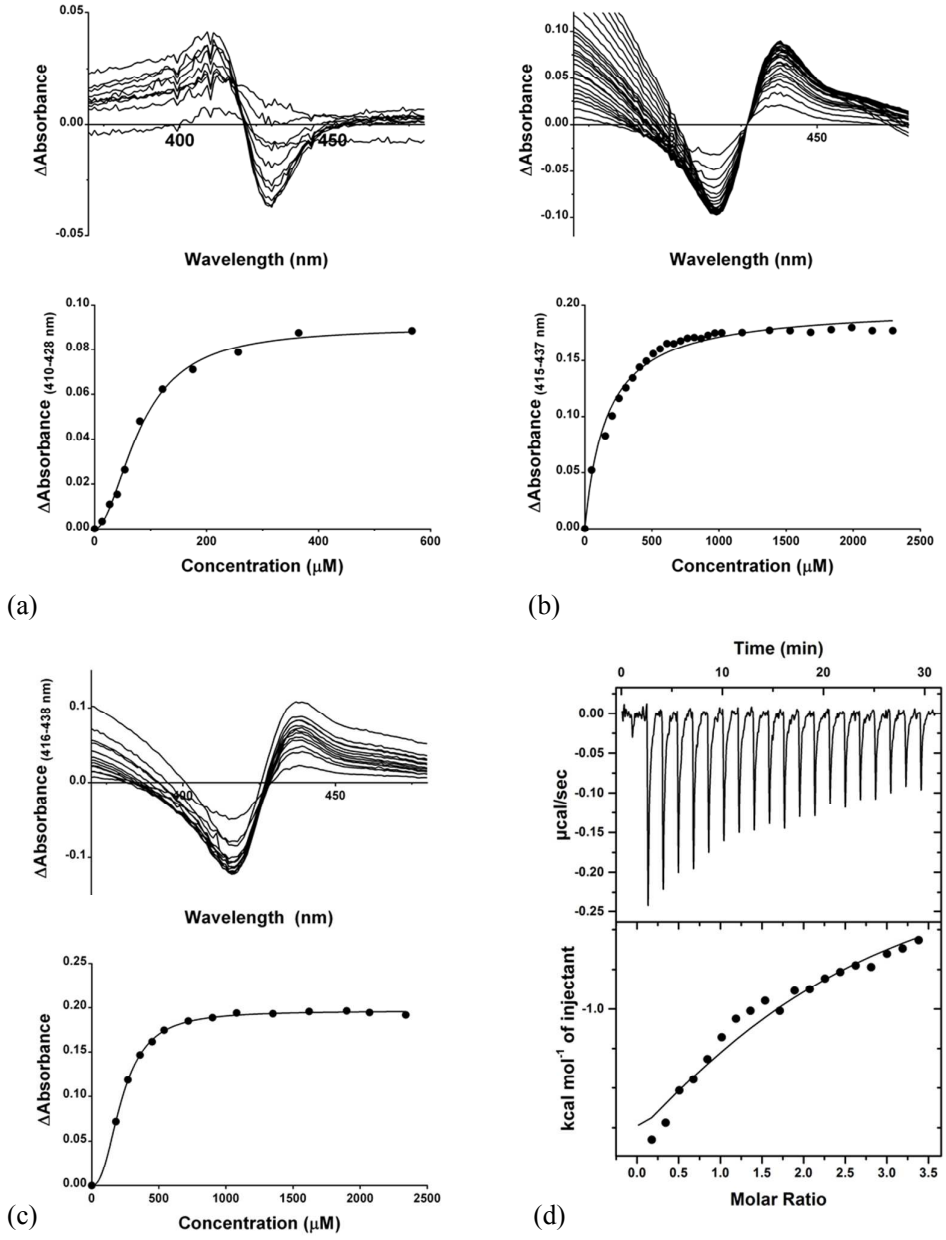

Figure S2. Binding affinity titrations. (a-c) Difference spectra (top panels) and concentration dependent change in absorbance (bottom panels) from the titration of CYP144A1 (6 μM) with (a) compound 1, (b) compound 2, and (c) compound 4. Data were fitted using the Hill equation for compound **1** (h = 1.8) and **4** (h = 2.4), or a hyperbolic function for compound **2**. (d) ITC binding isotherm for the titration of CYP144A1 (60 μM) with compound **3** (1 mM). The residual heat of ligand dilution was subtracted as a constant value. The integrated enthalpy change was fitted using a one-site binding model setting N = 2.

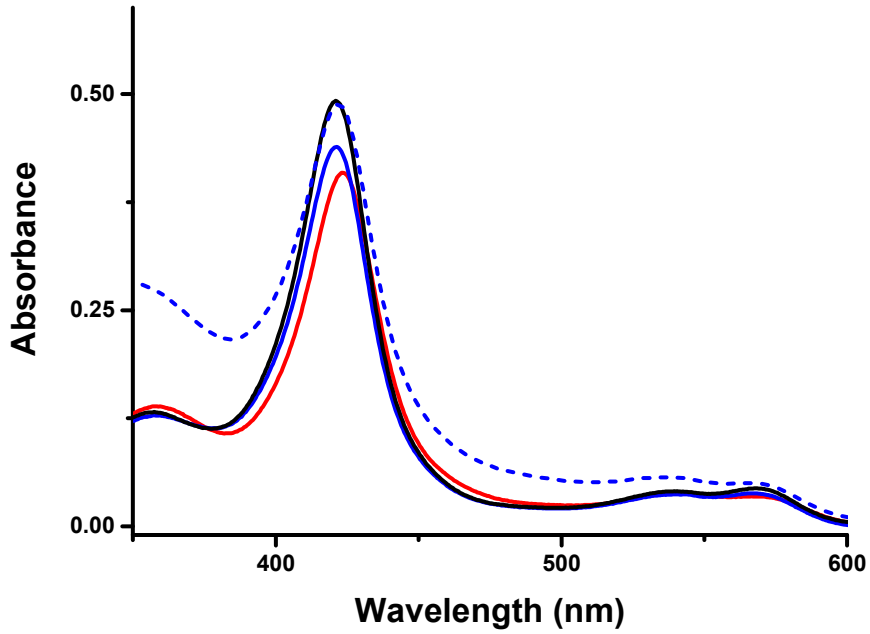

Figure S3. Competitive binding of compound **3** and econazole to CYP144A1. The Soret λ_{max} of the ligand-free CYP144A1 (black spectrum) at 421.0 nm is not affected by compound **3** (100 μM, blue spectrum). Econazole (50 μM, red spectrum) caused the Soret λ_{max} to red-shift to 423.5 nm, and the addition of compound **3** (50 μM, blue dashed spectrum) reduced this shift to 422.0 nm.

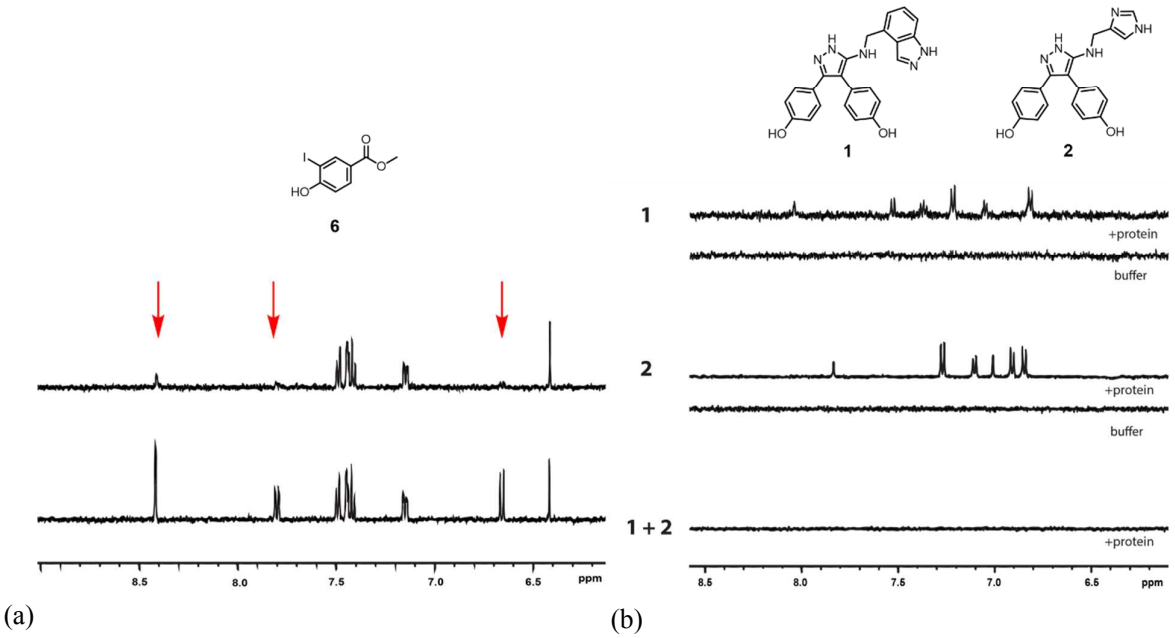

(a) (b)

Figure S4. Ligand-observed NMR screening and binding mode characterization. (a) CPMG spectra of a cocktail of 3 fragments (each 200 μM) in buffer (bottom spectrum) and in the presence of CYP144A1 (20 μM) (top spectrum). Red arrows indicate proton signals corresponding to the fragment hit identified as methyl 4-hydroxy-3-iodobenzoate **5**. (b) CPMG spectra of compound **1** (200 μM) and compound **2** (200 μM) tested independently in buffer and with CYP144A1 (20 μM) (top and middle set s of spectra); and also compound **1** and **2** tested in competition in the presence of CYP144A1 (20 μM) (bottom spectrum).